

Fault Impact Assessment on Indirect Field Oriented Control for Induction Motor

¹R.Senthil kumar, ² R.M.Sekar, ³ L.Hubert Tony Raj, ⁴ I.Gerald Christopher Raj

¹PG scholar, Department of EEE, PSNA College of Engineering & Technology Dindigul – 624 622, Tamilnadu, India.

²Associate Professor, Department of EEE, PSNA College of Engineering & Technology Dindigul – 624 622, Tamilnadu, India.

³PG scholar, Department of EEE, PSNA College of Engineering & Technology Dindigul – 624 622, Tamilnadu, India.

⁴Associate Professor, Department of EEE, PSNA College of Engineering & Technology Dindigul – 624 622, Tamilnadu, India.

ABSTRACT:

This paper presents an induction motor drives operating under indirect field-oriented control in which rotor flux DQ axis model is used. In this model, various faults are analyzed such as voltage, current, speed and torque, stator flux. To develop the model, faults are first identified, and then, a simulation model of the setup is developed. Faults are injected into the model in sequential levels and the system performance is assessed after each fault. Here rotor flux DQ model of induction motor is developed and it's controlled by using indirect field oriented control is studied. Here IFOC with DQ model was simulated using MATLAB/ SIMULINK software. Also the waveforms of voltage, current, speed, torque, Q axis and D axis stator flux are obtained. The above faults are analyzed and rectified which results in the increase of efficiency. This analysis is shown to be simple and useful for assessing the reliability of motor drives.

Keywords : Fault impact assessment, Induction motor drive, Rotor flux DQ axis model, openloop and closedloop IFOC

I. INTRODUCTION

Reliability assessment of motor drives is essential, especially in electric transportation applications. Safety is a major concern in such applications, and it is tied directly to re-liability. Induction machines, due to their reliability and low cost, are widely used in industrial applications. However, several electro-mechanical faults may occur during their life span. In industry, most failures interrupt a process and finally reduce or even stop the production. Thus, expensive scheduled maintenance is performed in order to prevent sudden failure and avoid economic damage[1].

The computer simulation for these various modes of operation is conveniently obtained from the equations which describe the symmetrical induction machine in an arbitrary reference frame [2]. As in Fig. 1[3] shows entire block diagram of induction motor drive. To control the rotor which creates torque equation is called as rotor flux DQ model. while faults in supply voltage that is affected on stator voltage. that is not affected on rotor voltage. Because rotor voltage produced due to electromagnetic induction principle. So rotor flux DQ model is used. stator and synchronous reference frame is applicable for squirrel cage induction motor[2]. because rotor part in short circuited in squirrel cage induction motor. The rotor reference frame is applicable for slip ring or

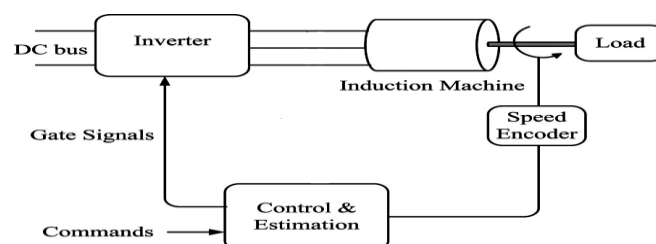


Fig. 1. Typical Induction Motor Drive

wound rotor induction motor. Here synchronous reference frame is presented. because while converting 3 phase to 2 phase which all parts considering DC quantity and control method is simple. The d-axis component is aligned with the rotor flux vector and regarded as the flux-producing current component. On the other hand, the q-axis current, which is perpendicular to the d-axis, is solely responsible for torque production. Based on the pioneering work of Blaschke, high performance induction motor drives have been developed in recent decades. The high dynamic performance is achieved using the field-orientation theory which requires controlling the stator current vector relative to the rotor flux [4]. The indirect field oriented control method is essentially the same as direct oriented control, except the unit vector signals are generated in feed forward manner [5]. Indirect field oriented control is very popular in industries IFOC being more commonly used because in closed-loop mode such drives more easily operate throughout the speed range from zero speed to high-speed field-weakening in DFOC, flux magnitude and angle feedback signals are directly calculated using so-called voltage or current models. In this paper, a complete framework for induction motor under indirect field oriented control (IFOC) is presented. Here cover the faults in voltage, current, speed, torque, Q and D axis stator flux. In this paper change the voltage and to study can be carried out to motor performance.

II. DYNAMIC MODEL OF INDUCTION MOTOR

The dynamic model model of squirrel cage induction motor [SEIM] in stationary reference frame in α - β reference frame variables [6].

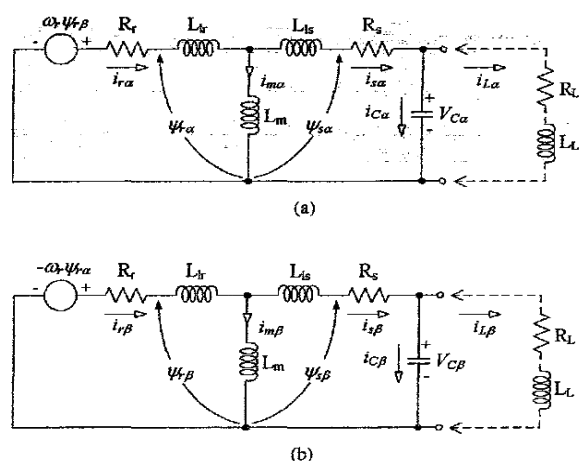


Fig. 2. Equivalent Circuit of SCIM (a) α axis (b) β axis

Components stator and rotor voltage of the induction motor can be expressed as follows:

$$V_{s\alpha} = R_s i_{s\alpha} + L_s \frac{d}{dt} i_{s\alpha} + L_m \frac{d}{dt} i_{r\alpha} \quad (1)$$

$$V_{s\beta} = R_s i_{s\beta} + L_s \frac{d}{dt} i_{s\beta} + L_m \frac{d}{dt} i_{r\beta} \quad (2)$$

$$0 = R_r i_{r\alpha} + L_r \frac{d}{dt} i_{r\alpha} + L_m \frac{d}{dt} i_{s\alpha} + \omega_r \Psi_{r\beta} \quad (3)$$

$$0 = R_r i_{r\beta} + L_r \frac{d}{dt} i_{r\beta} + L_m \frac{d}{dt} i_{s\beta} - \omega_r \Psi_{r\alpha} \quad (4)$$

The components of rotor flux linkage in the stationary reference can be written as

$$\Psi_{r\alpha} = L_m i_{s\alpha} + L_r i_{r\alpha} + \Psi_{r\alpha 0} \quad (5)$$

$$\Psi_{r\beta} = L_m i_{s\beta} + L_r i_{r\beta} + \Psi_{r\beta 0} \quad (6)$$

Where $\Psi_{r\alpha 0}$ and $\Psi_{r\beta 0}$ are the residual rotor flux linkages in α - β axis, respectively.

Then, with an electrical rotor speed of ω_r , the components of rotating voltage in the stationary reference frame are as the follows:

$$\omega_r \Psi_{r\alpha} = \omega_r L_m i_{s\alpha} + \omega_r L_r i_{r\alpha} + \omega_r \Psi_{r\alpha 0} \quad (7)$$

$$\omega_r \Psi_{r\beta} = \omega_r L_m i_{s\beta} + \omega_r L_r i_{r\beta} + \omega_r \Psi_{r\beta 0} \quad (8)$$

The expressions for capacitor voltages are,

$$V_{c\alpha} = \frac{1}{c} \int i_{c\alpha} dt + V_{c\alpha 0} \quad (9)$$

$$V_{c\beta} = \frac{1}{C} \int i_{c\beta} dt + V_{c\beta 0} \quad (10)$$

Using Fig. 2 equations (1)-(10), for the matrix equations of SCIM at no-load in the stationary reference frame are given by

$$\begin{bmatrix} 0 \\ 0 \\ 0 \\ 0 \end{bmatrix} = \begin{bmatrix} R_s + pL_s & 0 & pL_m & 0 \\ 0 & R_s + pL_s & 0 & pL_m \\ pL_m & \omega_r L_m & R_r + pL_r & \omega_r L_r \\ -\omega_r L_m & pL_m & -\omega_r L_r & R_r + pL_r \end{bmatrix} \begin{bmatrix} i_{s\alpha} \\ i_{s\beta} \\ i_{r\alpha} \\ i_{r\beta} \end{bmatrix} + \begin{bmatrix} V_{c\alpha} \\ V_{c\beta} \\ \omega_r \Psi_{r\beta 0} \\ -\omega_r \Psi_{r\alpha 0} \end{bmatrix} \quad (11)$$

From (11), can be written the state equations as follows:

$$A_p I_G + B I_G + V_G = 0 \quad (12)$$

Where,

$$A = \begin{bmatrix} L_s & 0 & L_m & 0 \\ 0 & L_s & 0 & L_m \\ L_m & 0 & L_r & 0 \\ 0 & L_m & 0 & L_r \end{bmatrix}, B = \begin{bmatrix} R_s & 0 & 0 & 0 \\ 0 & R_s & 0 & 0 \\ 0 & \omega_r L_m & R_r & \omega_r L_r \\ -\omega_r L_m & 0 & -\omega_r L_r & R_s \end{bmatrix}$$

$$I_G = \begin{bmatrix} i_{s\alpha} \\ i_{s\beta} \\ i_{r\alpha} \\ i_{r\beta} \end{bmatrix}, V_G = \begin{bmatrix} V_{c\alpha} \\ V_{c\beta} \\ \omega_r \Psi_{r\beta 0} \\ -\omega_r \Psi_{r\alpha 0} \end{bmatrix}$$

I. INDUCTION MOTOR MODEL IN DQ0 SYNCHRONOUS REFERENCE FRAMES

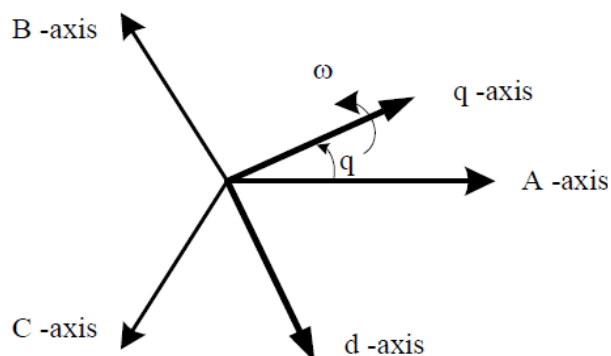


Fig. 3. Change of variables 3Φ to 2Φ conversion

Using Fig. 3[7] Synchronous frame induction motor equations are given as eqn 13 to eqn 17.

Stator $q^e d^e$ voltage equations:

$$v_{qs}^e = \frac{d\Psi_{qs}^e}{dt} + \omega_e \Psi_{ds}^e + r_s i_{qs}^e \quad (13)$$

$$v_{ds}^e = \frac{d\Psi_{ds}^e}{dt} - \omega_e \Psi_{qs}^e + r_s i_{ds}^e$$

Rotor $q^e d^e$ voltage equations:

$$v_{qr}^e = \frac{d\Psi_{qr}^e}{dt} + (\omega_e - \omega_r) \Psi_{dr}^e + r'_r i_{qr}^e \quad (14)$$

$$v_{dr}^e = \frac{d\Psi_{dr}^e}{dt} - (\omega_e - \omega_r) \Psi_{qr}^e + r'_r i_{dr}^e$$

Where,

$$\begin{bmatrix} \Psi_{qs}^e \\ \Psi_{ds}^e \\ \Psi_{qr}^e \\ \Psi_{dr}^e \end{bmatrix} = \begin{bmatrix} L_s & 0 & L_m & 0 \\ 0 & L_s & 0 & L_m \\ L_m & 0 & L'_r & 0 \\ 0 & L_m & 0 & L'_r \end{bmatrix} \begin{bmatrix} i_{qs}^e \\ i_{ds}^e \\ i_{qr}^e \\ i_{dr}^e \end{bmatrix} \quad (15)$$

Torque Equations:

$$T_{em} = \frac{3}{2} \frac{p}{2} (\Psi_{qr}^e i_{dr}^e - \Psi_{dr}^e i_{qr}^e) Nm \quad (16)$$

III. INDIRECT FIELD ORIENTED CONTROL OF INDUCTION MOTOR

Fig. 4 shows the block diagram of indirect field orientation control strategy with sensor in which speed regulation is possible using a control loop.

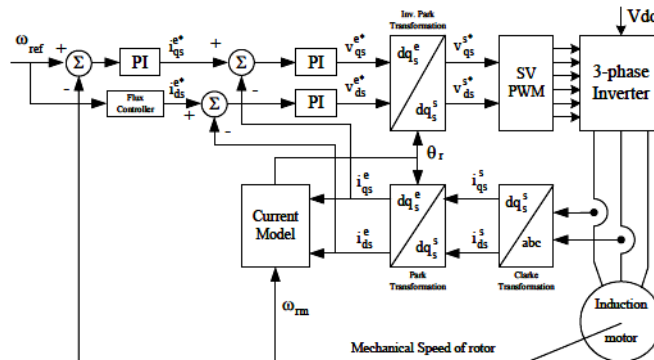


Fig. 4. Indirect Field-Oriented Control for Induction Motor Drives

In IFOC, flux space angle feed forward and flux magnitude signals first measure stator currents and rotor speed for then deriving flux space angle proper by summing the rotor angle corresponding to the rotor speed and the calculated reference value of slip angle corresponding to the slip frequency. An induction motor drive under IFOC requires measurements of the three-phase currents and speeds and has two control inputs for torque, or speed, and rotor flux[8].

$$p\lambda_{dr}^e + \frac{r_r}{L_r} \lambda_{dr}^e - \frac{r_r}{L_r} L_m i_{ds}^e = 0 \text{ steady state } i_{ds}^e = \frac{\lambda_{dr}^e}{L_m} \quad (17)$$

$$\omega_{slip} = \frac{r_r}{\lambda_r} \left(\frac{L_m}{L_r} \right) i_{qs}^e = \frac{L_m i_{qs}^e}{\lambda_r \lambda_r} \quad (18)$$

$$i_{qs}^e = - \frac{L_m}{L_m + L_{lr}} i_{qs}^e \quad (19)$$

$$T_e = \frac{3}{2} \frac{p}{2} \frac{L_m}{L_r} \lambda_d i_{qs}^e \quad (20)$$

The reference currents of the q-d-o axis (i_{qs}^e, i_{ds}^e) are converted to the reference phase voltages (v_{qs}^e, v_{ds}^e) as the commanded voltages for the control loop. By using ω_{slip} , which is shown in equation(17) and using actual rotor speed, the rotor flux position is obtained.

$$\int_0^t \omega_{slip} dt + \int_0^t \omega_{re} dt = \theta_r(t) \quad (21)$$

or

$$\int_0^t \omega_{slip} dt + \int_0^t \theta_{re} dt = \theta_r(t) \quad (22)$$

As shown in Fig. 4., two-phase current feeds the Clarke transformation block. These projection outputs are indicated as i_{ds}^s and i_{qs}^s . These two components of the current provide the inputs to Park's transformation, which gives the currents in qds^e the excitation reference frame. The i_{ds}^e and i_{qs}^e components, which are outputs of the Park transformation block, are compared to their reference values i_{ds}^e , the flux reference, and i_{qs}^e , the torque reference. The torque command, i_{qs}^e , comes from the output of the speed controller. The flux command, i_{ds}^e , is the output of the flux controller which indicates the right rotor flux command for every speed reference. Magnetizing current i_{ds}^e is usually between 40 and 60% of the nominal current. For operating in speeds above the nominal speed, a field weakening section should be used in the flux controller section. The current regulator outputs, v_{ds}^e and v_{qs}^e are applied to the inverse Park transformation. The outputs of this block are the signals that drive the inverter.

IV. MOTOR DRIVE, FAULTS AND PERFORMANCE

A. System Overview

As in Fig. 4 faults can occur in the following six possible subsystems or components:

- [1] Faults due to voltage variations
- [2] Faults due to current variations
- [3] Faults due to speed variations
- [4] Faults due to load torque variations
- [5] Faults due to Q axis Stator Flux Variations
- [6] Faults due to D axis Stator Flux Variations

B. Voltage Variation

In this paper to change the voltage and to study can be carried out to motor performance. To control the induction motor by using indirect field oriented control method. Many problems are a result of high or low voltage, unbalanced voltage, ungrounded power systems, or voltage spikes[9].

V. SIMULATION AND EXPERIMENTS

Some of the faults could damage the experimental setup and cannot be tested directly. Also, many commercial motor drives have built-in protection circuitry and algorithms that take action after a fault by shutting down or otherwise altering operation. It is not easy (or advisable) to override protection, but fault modes used here can also integrate protection in several aspects.. Even though the simulations here do not model or cover all physical dynamics, noise, vibration, power loss, and nonlinearities of material, they provide a useful tool that can save the cost of rebuilding a motor drive, or most other systems, after severe failures.

A. Simulations

Simulations provide a safe environment to evaluate even the most extreme faults, provided a simulation has been validated in hardware. Some commercial drives have fault detection and isolation, which would not be helpful if the target is to observe drive performance under faults, Simulations of the IFOC induction motor drive shown in Fig. 4 were performed in MATLAB/SIMULINK for a 1.5-hp induction machine. The inverter involved IGBT–diode pairs from the SimPowerSystems Toolbox in SIMULINK. For the implementation of the state space equations of a system model, MATLAB/ SIMULINK. has the denominated user defined functions or s-functions [10]. In these blocks the code that defines the model in state equations can be written. In this code so much is defined the number of inputs and outputs, like the states and the state space equations of the system. This s-function will correspond to a block with the inputs, outputs and parameters shown in Fig. 5. The s-function can be called from a MATLAB/SIMULINK s-function block. In Fig. 5, one is the SIMULINK block diagram where “VSI-IM model” is the s-function that call’s the defined function. The inputs are multiplexed in a bus can be demultiplexed, and the same occurs for the outputs. Here rotor flux DQ model of induction motor is presented in programmed manner by using M-File. and fault analysis also written in the same M-File. While changing the voltage it will affect current, speed, torque and flux.

TABLE I. MACHINE PARAMETERS

Sl.no	Machine Parameters in perunit	
1	Stator resistance	$R_s = 0.01$
2	Rotor resistance	$R_r = 0.02$
3	Stator leakage inductance	$L_{sl} = 0.1$
4	Rotor leakage inductance	$L_{rl} = 0.1$
5	Magnetizing inductance	$L_m = 4.5$
6	Load torque	$T_l = 0.2375$
7	Supply voltage	$V_s = 1.0$

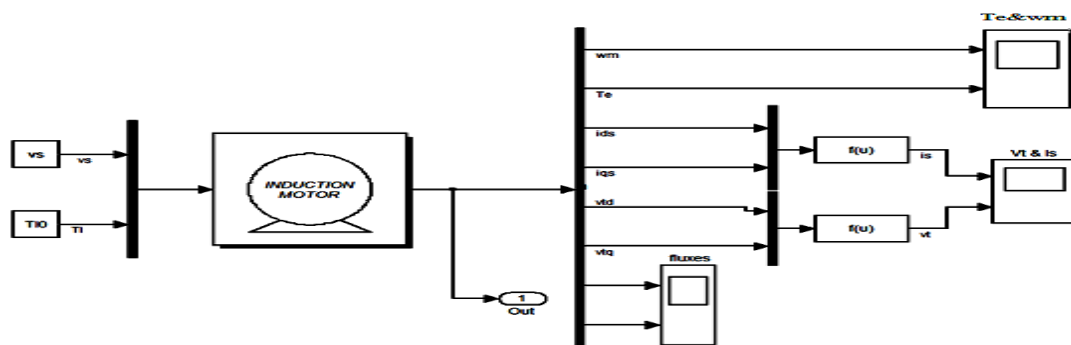


Fig. 5. Simulation Diagram of Induction Motor Under Open Circuit Condition

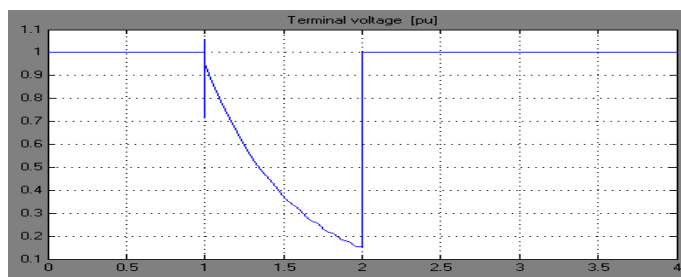


Fig 6. Voltage Response of Induction Motor Under Fault Condition

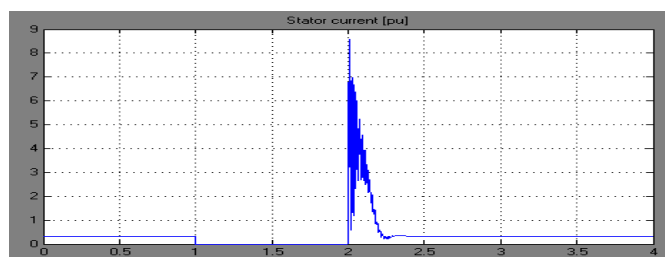


Fig. 7. Current Response of Induction Motor Under Fault Condition

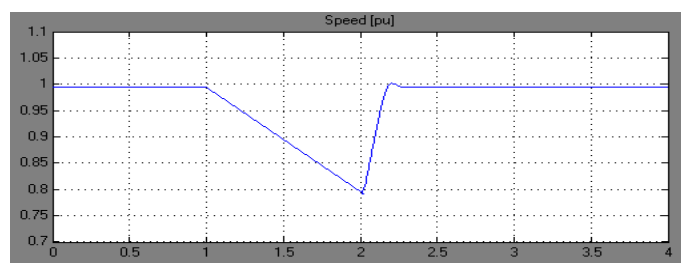


Fig. 8. Speed Response of Induction Motor Under Fault Condition

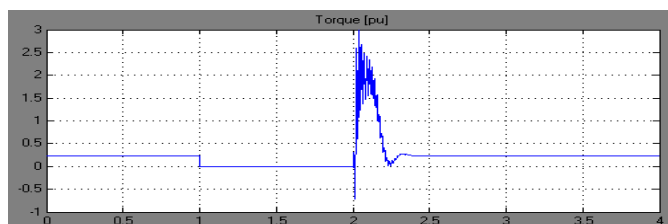


Fig 9. Load Torque Response of Induction Motor Under Fault Condition

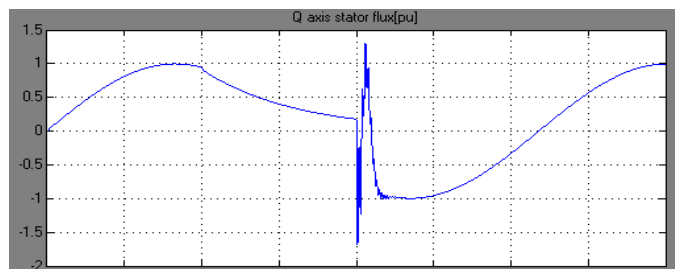


Fig. 10. Q axis Stator Flux Response of Induction Motor Under Fault Condition

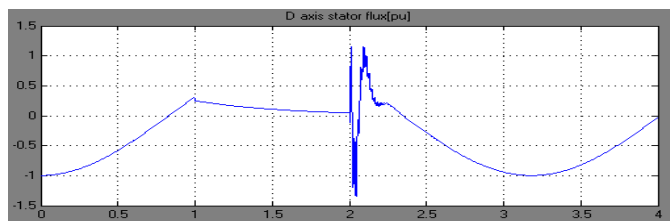


Fig. 11. D axis Stator Flux Response of Induction Motor Under Fault Condition

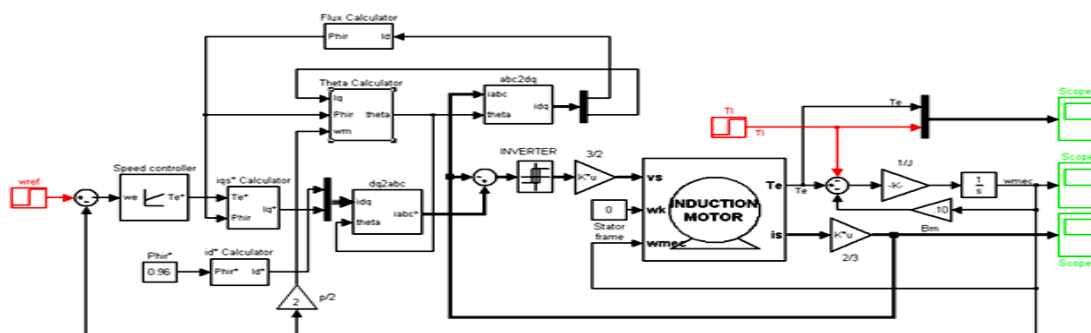


Fig. 12. Simulation Diagram of Closed loop IFOC

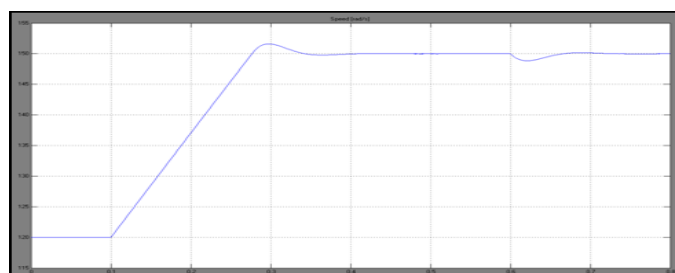


Fig. 13. Speed Response of Induction Motor Under Normal Condition

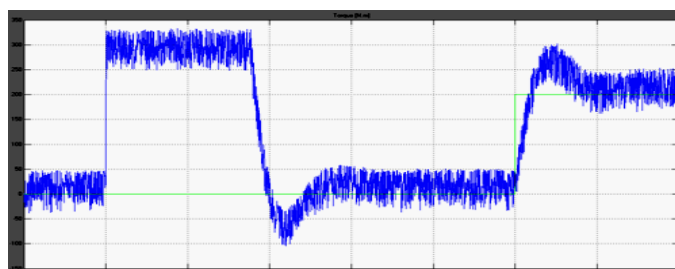


Fig. 14. Torque Response of Induction Motor Under Normal Condition

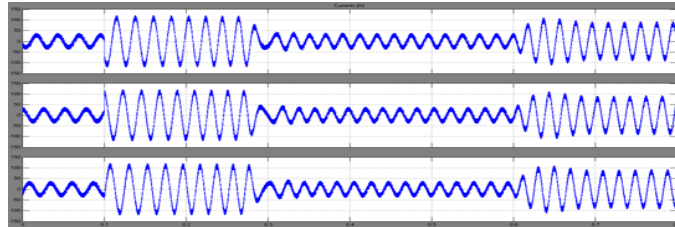


Fig. 15. Currents Response of Induction Motor Under Normal Condition

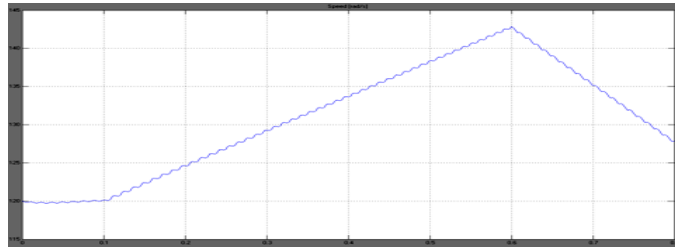


Fig. 16. Speed of Induction Motor Under Fault Condition

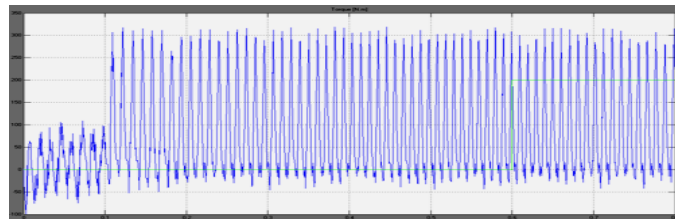


Fig. 17. Torque Response of Induction Motor Under Fault Condition

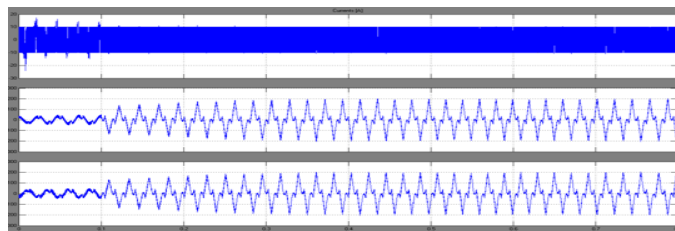


Fig. 18. Currents Response of Induction Motor Under Fault Condition

B. Simulation Results

The drive architectures of Fig.5 have been completely implemented and assessed in the , MATLAB/SIMULINK environment along with their respective control systems. The simulation is based on the parameters shown in Table I. A simulation study based on the model shown in Fig. 6 is carried out to compare open loop IFOC. The following figures shows waveforms of voltage, current, speed, torque and flux under fault conditions. As in Fig. 6, at normal condition there is no disturbance between 0 to 1. when the fault occurs at point 1, suddenly the voltage was dipped between 1 to 2. After 2, the fault was recovered so it maintain steady state condition. As in Fig. 7, at normal condition there is no disturbance between 0 to 1. when the fault occurs at point 1 suddenly the current was reached 0 between 1 to 2. After 2, the fault was recovered, in that point suddenly the current was increased more than rated current. Because current transients will occur. so it reaches steady state at 2.2. As in Fig. 8, at normal condition there is no disturbance between 0 to 1. when the fault occurs at point 1, suddenly the voltage was decreased between 1 to 2. After 2, the fault was recovered, in that point the speed not reaches steady state at point 2. It takes some time to reach steady state. So it reaches steady state at 2.2. As in Fig. 9, at normal condition there is no disturbance between 0 to 1. when the fault occurs at point 1 suddenly the torque was reached 0 between 1 to 2. After 2, the fault was recovered, in that point suddenly the torque was increased more than rated torque. so oscillations will occur. It takes some time to reach steady state. So it reaches steady state at 2.2. As in Fig. 10, at normal condition there is no disturbance between 0 to 1.

when the fault occurs at point 1 suddenly the Q axis stator flux was reached 0 between 1 to 2. After 2, the fault was recovered, in that point suddenly the flux was increased more than rated flux. so oscillations will occur. It takes some time to reach normal state. So it reaches steady state at 2.2. As in Fig. 11, at normal condition there is no disturbance between 0 to 1. when the fault occurs at point 1 suddenly the D axis stator flux was reached 0 between 1 to 2. After 2, the fault was recovered, in that point suddenly the flux was increased more than rated flux. so oscillations will occur. It takes some time to reach normal state. So it reaches steady state at 2.2.

C. Experimental Environment

The experimental setup includes all control, power electronics, motor, load, and measurements. The control and some measurements are available on an eZdspF2812 platform which is based on a Texas Instruments TMS320F2812 DSP. This control platform is integrated into the Grainger Center Modular Inverter [11] which also includes an inverter power stage rated at 400V and 100A. A dynamometer is used to set the load torque. Measurements include speed, torque, currents, voltages, and input and output power. All control and measurement devices, including the dynamometer, are controlled using MATLAB/ Simulink through the Simulink Real-Time Workshop. Communication between the software and the DSP occurs through real-time data exchange (RTDX) via a parallel port. Here fault monitoring kit is also needed to analyze various faults. There are two factors are considered. The first factor is to avoid injecting faults that could cause severe failures or trigger the protection circuitry as predicted from simulations. The second factor is to use a tight external closed-loop torque control in experiments to avoid sudden overload conditions on the dynamometer and the motor shaft. The experimental setup is shown in Fig. 13,

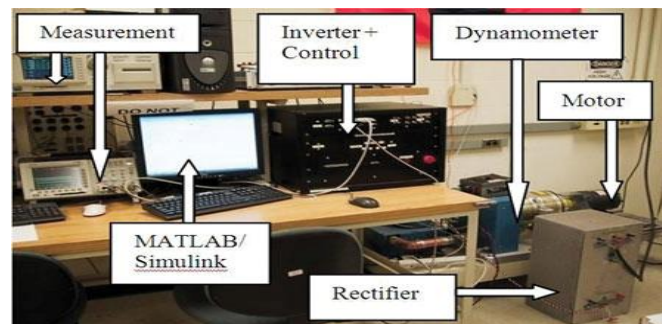


Fig. 19. Experimental setup for model validation.

VI. CONCLUSION

The Existing methodology for reliability modeling covers essential faults in a drive system, including the machine, power electronics converters, and sensors. The methodology leads to rotor flux DQ model of an induction motor drive under open loop IFOC and can be extended to other drives or to more faults in other components. A model was validated in experiments and used for the complete procedure. The survivor function of the complete system was found analytically including fault coverage. Simplifications were proposed based on dominant fault modes, which were found to be faults in the voltage, current, speed, load torque and stator flux. Further research could apply this methodology to other drive topologies, more components in any topology (e.g., link capacitors, gate drives, etc.), design of fault tolerance, and actual field failure rates. Even though DQ's model might not be accurate since faults generally vary with time, the proposed methodology serves the purpose of a comprehensive, straightforward, and versatile reliability modeling procedure. Thus the open loop and closed loop IFOC with DQ model is simulated using MATLAB/ SIMULINK.

REFERENCES

- [1] Ali. M. Bazzi, Alejandro Dominguez-Garcia, and Philip T. Krein, "Markov Reliability Modeling for Induction Motor Drives Under Field-Oriented Control," IEEE Trans. Power Electron., Vol, No. 2, feb 2012.
- [2] P. C Krause and C. H Thomas, "Simulation of Symmetrical Induction Machinery" IEEE Trans., Power Apparatus and Systems Vol. PAS-84, No. 11, 1965
- [3] A. M. Bazzi, A. D. Dominguez-Garcia, and P. T. Krein "A method for impact assessment of faults on the performance of field oriented control drives: A first step to reliability modeling" in Proc. IEEE Appl. power Electron. Conf. Expo., 2010, pp. 256-263
- [4] Zsolt Beres and Peter Vranka, "Sensor less IFOC of Induction Motor With Current Regulators in Current Reference Frame" IEEE Trans. Ind. Appl., Vol. 37, No.4, 2001.
- [5] Alfio consoli, Giuseppe Scarcella and Antonio Testa, "Slip Frequency Detection for Indirect Field Oriented Control Drives" IEEE Trans. Ind. Appl., Vol, No.1., 2004.

- [6] G. R. Slemon, "Modeling of Induction Machines for Electric Drives" IEEE Trans. Ind. Appl., Vol. 25, No.6, pp. 1126-1131, Nov/Dec 1989.
- [7] S. Green, D. J. Atkinson, A. G. Jack, B. C. Mecrow, and A. King, "Sensorless operation of a Fault Tolerant PM Drive," IEE Proc. Elect. Power Appl., Vol. 150, No.2, pp.117-125, Mar. 2003
- [8] Naceri Farid, Belkacem Sebti, Kercha Memberka and Benmokrane Tayed, "Performance Analysis of Field-Oriented Control and Direct Torque Control for Sensorless Induction Motor Drives" in Proc. 15th Mediterranean Conf., on Control & Automation, July 2007.
- [9] W. R. Finley, M. M. Hodowanec, W.G. Holter, "An Analytical Approach to Solving Motor Vibration Problems" IEEE PCIC Conf., Sep 1999.
- [10] Bin Wu, S. B. Dewan and G. R. Slemon, "PWM CSI Inverter Induction Motor Drives" IEEE Trans. Ind. Appl., Vol.28, No.1, pp 64-71, 1992
- [11] J. Kimball, M. Amerhein, A. Kwansinki, J. Mossoba, B. Nee, Z. Sorchini, W. Weaver, J. Weels and G. Zhang, "Modular Inverter for Advanced Control Applications" Technical Report CEME-TR-200-01, University of Illinois May 2006.